Article

Alloyed Semiconductor Quantum Dots: Tuning the Optical Properties without Changing the Particle Size

Robert E. Bailey, and Shuming Nie

J. Am. Chem. Soc., **2003**, 125 (23), 7100-7106• DOI: 10.1021/ja035000o • Publication Date (Web): 16 May 2003

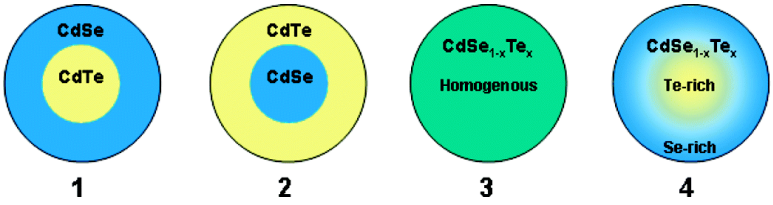

More About This Article

Additional resources and features associated with this article are available within the HTML version:

- Supporting Information
- Links to the 46 articles that cite this article, as of the time of this article download
- Access to high resolution figures
- Links to articles and content related to this article
- Copyright permission to reproduce figures and/or text from this article

View the Full Text HTML

J|A|C|S
ARTICLES
Published on Web 05/16/2003

Alloyed Semiconductor Quantum Dots: Tuning the Optical Properties without Changing the Particle Size

Robert E. Bailey and Shuming Nie*

Contribution from the Departments of Biomedical Engineering and Chemistry, Emory University and Georgia Institute of Technology, 1639 Pierce Drive, Suite 2001, Atlanta, Georgia 30322

Received March 5, 2003; E-mail: snie@emory.edu

Abstract: Alloyed semiconductor quantum dots (cadmium selenium telluride) with both homogeneous and gradient internal structures have been prepared to achieve continuous tuning of the optical properties without changing the particle size. Our results demonstrate that composition and internal structure are two important parameters that can be used to tune the optical and electronic properties of multicomponent, alloyed quantum dots. A surprising finding is a nonlinear relationship between the composition and the absorption/emission energies, leading to new properties not obtainable from the parent binary systems. With red-shifted light emission up to 850 nm and quantum yields up to 60%, this new class of alloyed quantum dots opens new possibilities in band gap engineering and in developing near-infrared fluorescent probes for in vivo molecular imaging and biomarker detection.

Size-tunable properties have become a hallmark of quantum dots and related nanostructures.[1,2] These properties are currently under intensive study for potential use in optoelectronics, high-density memory, quantum-dot lasers, and lately for biosensing and biolabeling.[3−9] Recent advances have led to the development of colloidal nanostructures including core−shell quantum dots,[10−12] elongated quantum rods,[13] doped magnetic nanoparticles,[14−16] quantum-dot quantum-well (QDQW) heterostructures,[17,18] and mixed semiconductor dots.[19,20] However, the tuning of electronic, optical, and magnetic properties by changing the particle size could cause problems in many applications such as nanoelectronics, superlattice structures, and biological labeling. In this paper, we report a new class of alloyed semiconductor quantum dots (ternary CdSeTe) for continuous tuning of quantum confinement without changing the particle size. We show that both the alloy composition (the Se:Te molar ratio) and the internal structure can be controlled in a single step by varying the relative amounts of the starting materials.

On the basis of the particle-in-a-sphere models for quantum dots,[21,22] the composition effect arises from a strong dependence of the electronic energies on the effective exciton mass (reduced mass of a coupled hole/electron pair). The other key parameter in quantum confinement is the particle size, as has been discussed in the literature.[1,2] Theoretical calculations using the effective mass approximation (EMA)[21,22] and atomistic pseudopotential methods[23,24] have successfully explained the optical and electronic spectra of both spherical quantum dots and elongated quantum rods.[25] Experiment measurements based on the Hall effect and optical reflectivity[26,27] have shown that the effective exciton mass (8.6% of the free electron mass) in CdTe is ca. 20% smaller than that in CdSe. Thus, the effective exciton mass in ternary CdSeTe alloys should be modulated by the alloy composition, possibly in the form of a linear relationship between the exciton mass and composition. Surprisingly, our experimental data reveal that the exciton mass in the alloyed CdSeTe nanocrystals can be substantially lower than that in pure

(1) Murray, C. B.; Kagan, C. R.; Bawendi, M. G. *Annu. Rev. Mater. Sci*. **2000**, *30*, 545−610.
(2) Alivisatos, A. P. *Science* **1996**, *271*, 933−937.
(3) Bruchez, M., Jr.; Moronne, M.; Gin, P.; Weiss, S.; Alivisatos, A. P. *Science* **1998**, *281*, 2013−2015.
(4) Chan, W. C. W.; Nie, S. M. *Science* **1998**, *281*, 2016−2018.
(5) Akerman, M. E.; Chan, W. C. W.; Laakkonen, P.; Bhatia, S. N.; Ruoslahti, E. *Proc. Natl. Acad. Sci. U.S.A.* **2002**, *99*, 12617−12621.
(6) Dubertret, B.; Skourides, P.; Norris, D. J.; Noireaux, V.; Brivanlou, A. H.; Libchaber, A. *Science* **2002**, *298*, 1759−1762.
(7) Wu, X.; Liu, H.; Liu, J.; et al. *Nat. Biotechnol.* **2003**, *21*, 41−46.
(8) Jaiswal, Y. K.; Mattoussi, H.; Mauro, J. M.; Simon, S. M. *Nat. Biotechnol*. **2003**, *21*, 47−51.
(9) Murphy, C. J. *Anal. Chem*. **2002**, *74*, 520A−526A.
(10) Dabbousi, B. O.; Rodriguez-Viejo, J.; Mikulec, F. V.; Heine, J. R.; Mattoussi, H.; Ober, R.; Jensen, K. F.; Bawendi, M. G. *J. Phys. Chem. B* **1997**, *101*, 9463−9475.
(11) Peng, X. G.; Schlamp, M. C.; Kadavanich, A. V.; Alivisatos, A. P. *J. Am. Chem. Soc*. **1997**, *119*, 7019−7029.
(12) Cao, Y. W.; Banin, U. *J. Am. Chem. Soc*. **2000**, *122*, 9692−9702.
(13) Peng, X. G.; Manna, L.; Yang, W. D.; Wickham, J.; Scher, E.; Kadavanich, A.; Alivisatos, A. P. *Nature* **2000**, *404*, 59−61.
(14) Nanif, K. M.; Meulenberg, R. W.; Strouse, G. F. *J. Am. Chem. Soc*. **2002**, *124*, 11495−11502.
(15) Mikulec, F. V.; Kuno, M.; Bennati, M. et al. *J. Am. Chem. Soc*. **2000**, *122*, 2532−2540.
(16) Counio, G.; Gacoin, T.; Boilot, J. P. *J. Phys. Chem. B* **1998**, *102*, 5257−5260.
(17) Mews, A.; Eychmuller, A.; Giersig, M. et al. *J. Phys. Chem*. **1994**, *98*, 934−941.
(18) Little, R. B.; El-Sayed, M. A.; Bryant, G. W.; et al. *J. Chem. Phys*. **2001**, *114*, 1813−1822.
(19) Korgel, B. A.; Monbouquette, H. G. *Langmuir* **2000**, *16*, 3588−3594.
(20) Rogach, A. L.; Harrison, M. T.; Kershaw, S. V.; Kornowski, A.; Burt, M. G.; Eychmuller, A.; Weller, H. *Phys. Stat. Solidi B* **2001**, *224*, 153−158.
(21) Efros, A. L.; Rosen, M.; Kuno, M.; Nirmal, M.; Norris, J. D.; Bawendi, M. G. *Phys. Rev. B* **1996**, *54*, 4843−4856.
(22) Efros, A. L. *Phys. Rev. B* **1992**, *46*, 7448−7458.
(23) Franceschetti, A.; Zunger, A. *Phys. Rev. B* **2000**, *62*, 2614−2623.
(24) Franceschetti, A.; Zunger, A. *Phys. Rev. Lett*. **1997**, *78*, 915−918.
(25) Hu, J. T.; Wang, L. W.; Li, L. S.; Yang, W. D.; Alivisatos, A. P. *J. Phys. Chem. B* **2002**, *106*, 2447−2452.
(26) Wheele, S.; Dimmock, J. O. *Phys. Rev*. **1962**, *125*, 1805−1815.
(27) Marple, D. T. F. *Phys. Rev*. **1963**, *129*, 2466−2470.

10.1021/ja035000o CCC: $25.00

CdSe or CdTe nanocrystals of the same size. Observed as a "depression" in both the excitonic absorption and the band-edge emission energies, this nonlinear effect leads to new optical and electronic properties that are not available from the parent binary quantum dots.

Materials and Methods

Materials. Cadmium oxide (CdO, 99.99%), selenium shot (Se, 99.999%), tri-*n*-octylphosphine (TOP, 90%), tri-*n*-octylphosphine oxide (TOPO, 90%), and hexadecylamine (HDA, 90%) were purchased from Aldrich (Milwaukee, WI). Tellurium powder (Te, 99.999%) was purchased from Alfa Aesar (Ward Hill, MA). Carbon-coated copper grids (200 mesh) for preparing TEM specimens were purchased from Electron Microscopy Sciences (Fort Washington, PA). A selenium stock solution (0.4 M) was prepared by dissolving 0.79 g of selenium shot in 25 mL of TOP, yielding a colorless solution. A tellurium stock solution at the same concentration was prepared by dissolving 1.28 g of tellurium powder in 25 mL of TOP, yielding a yellow saturated solution which required gentle heating before use in order to dissolve the remaining tellurium powder.

Synthesis of Alloyed Quantum Dots. Our strategy for preparing high-quality alloyed quantum dots was inspired by the original organometallic procedure,[28] the use of cadmium oxide as an inexpensive precursor,[29] and the report of mixed HDA−TOPO solvents for improved size monodispersity and fluorescence quantum yields.[30] Thus, a 125 mL round-bottom flask containing 9 g of TOPO, 3 g of HDA, and 16 mg of CdO was heated to ∼150 °C and was degassed under a vacuum of 20 Pa for 15 min. The flask was then filled with argon gas, and its temperature was increased to 325 °C. After the precursor CdO was dissolved completely in the solvent, the temperature was lowered to 300 °C and was allowed to stabilize for several minutes. For convenient control of reagent molar ratios, five premixed Se and Te solutions were prepared from the individual stock solutions at 0.4 M total concentration, but with Se:Te molar ratios of 100:0, 75:25, 50:50, 25:75, or 0:100. To prepare homogeneous alloyed quantum dots under cadmium-limited conditions (see discussion in next section), a premixed Se and Te solution in the amount of 2.5 mL (1.0 mmol) was rapidly injected (less than 1 s) into the colorless TOPO/HDA/CdO solution at 300 °C. The reaction mixture contained ca. 0.12 mmol of cadmium, approximately 8-fold less than the total amount of injected Se and Te. Aliquots of the reaction mixture were taken at 10 s intervals during the first 60 s, and then at longer intervals after the initial injection of the premixed Se and Te stock solution. The sampling aliquots were quenched in cold (25 °C) chloroform in order to stop further growth of the particles. To prepare gradient quantum dots under cadmium-rich conditions, about 2.5 mL (0.25 mmol) of a premixed Se and Te stock solution (diluted 4-fold) was injected into a colorless TOPO/HDA solution containing 2.0 mmol of cadmium at 300 °C. Under these conditions, the cadmium precursor was about 8-fold in excess of the total amount of injected Se and Te.

Synthesis of Core−Shell Quantum Dots. To synthesize core−shell nanocrystals with overall sizes and compositions similar to those of the alloyed quantum dots, we first calculated the core sizes and shell thicknesses that needed to be synthesized. Using either the crystal lattice parameters or the bulk densities of CdSe and CdTe, the calculated results were in agreement within 5%. Next, we synthesized the cores and monitored their growth by absorption spectroscopy, based on the known size-dependent behavior for CdSe and CdTe nanocrystals. When the desired core size was achieved, growth was stopped by quenching the reaction. The nanocrystals were isolated by precipitation with methanol and were placed into a new reaction flask containing TOPO, HDA, and additional CdO for shell growth. Shells were grown by dropwise addition of the desired stock solution to form the appropriate shell material (either 0.04 M Se or Te in TOP). Aliquots were taken out of the reaction mixture periodically for determination of particle size and elemental composition. The detailed procedures and reaction conditions were similar to those for the alloyed dots. All quantum dots were purified by several rounds of precipitation and centrifugation and were stored at room temperature for later characterization and use.

Characterization. UV−vis absorption spectra were recorded on a Shimadzu UV-2401PC scanning spectrophotometer operating at a slit width of 1.0 nm. Band gap energy determinations were made by analyzing the absorption data using the method outlined by Fendler and co-workers[31] to extract the value for the absorption onset. Photoluminescence spectra were acquired on a Spex FluoroMax spectrometer. Emission spectra were taken using an excitation wavelength of 475 nm with excitation and emission slit widths set at 2.0 nm. Recorded spectra were corrected for the wavelength dependence of detector response. The optical densities of all samples were adjusted to between 0.10 and 0.15 at the excitation wavelength, and quantum yield measurements were made by comparing the integrated nanocrystal emission in chloroform with that of fluorescent dyes (Atto 565 and Atto 680, Fluka, Milwaukee, WI) in ethanol. Transmission electron micrographs were obtained on a JEOL 1210 electron microscope operating at an accelerating voltage of 90 kV. Samples were prepared by placing a dilute solution of nanocrystals in chloroform onto carbon-coated copper grids and allowing them to dry in a vacuum desiccator overnight.

Energy-dispersive X-ray (EDX) data were acquired on a Philips XL30 ESEM-FEG equipped with an EDAX light element detector and processed on an EDAX Phoenix X-ray Microanalysis System. X-ray diffraction data were obtained from powder samples of $CdSe_{1-x}Te_x$ nanocrystals, which were first precipitated in chloroform with methanol followed by centrifugation to isolate a nanocrystal pellet. After the supernatant was discarded, each pellet was allowed to dry overnight and then was crushed into a fine powder which was sealed in a 0.5 mm capillary and mounted on the platform goniometer such that the capillary axis was coincident with the main instrument axis. Data were collected using Mo Kα radiation with a weighted mean wavelength of 0.71073 Å. The samples were continuously oscillated through 179° about the instrument axis during a 90-s data collection period. Data were recorded with a Bruker-AXS SMART6000 two-dimensional CCD detector diffraction system and processed with Bruker's SMART and GADDS software to produce the standard intensity vs diffraction angle data to a maximum diffraction angle of 39.5°.

Results and Discussion

Reaction Kinetics. Previous studies of binary quantum dots and bulk semiconductors have found that CdSe and CdTe nanocrystals can be prepared under similar conditions[29,32] and that these two semiconductors form homogeneous alloys at all proportions.[33] However, recent research (R. Bailey and S. Nie, unpublished data) indicates that elemental tellurium is considerably more reactive than selenium toward cadmium under rapid nucleation and growth conditions. Because of this difference in reactivity, the CdTe growth rate is approximately 2 times that of CdSe. Here we have taken advantage of these factors and have developed a novel procedure that allowed us to prepare two distinct types of alloyed semiconductor quantum dots. Specifically, all reagents are added into a "single pot", with a

(28) Murray, C. B.; Norris, D. J.; Bawendi, M. G. *J. Am. Chem. Soc.* **1993**, *115*, 8706−8715.
(29) Peng, Z. A.; Peng, X. G. *J. Am. Chem. Soc*. **2001**, *123*, 183−184.
(30) Talapin, D. V.; Rogach, A. L.; Kornowski, A.; Haase, M.; Weller, H. *Nano Lett.* **2001**, *1*, 207−211.
(31) Tian, Y.; Newton, T.; Kotov, N. A.; Guldi, D. M.; Fendler, J. H. *J. Phys. Chem.* **1996**, *100*, 8927−8939.
(32) Talapin, D. V.; Rogach, A. L.; Mekis, I.; Haubold, S.; Kornowski, A.; Haase, M.; Weller, H. *Colloid Surf. A* **2002**, *202*, 145−154.
(33) Willardson, R. K., Goering, H. L., Eds.; *Compound Semiconductors*; Reinhold: New York, 1962.

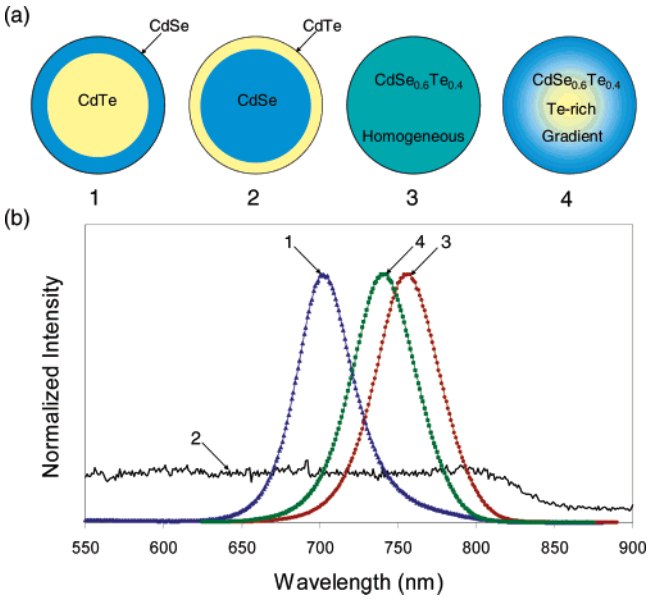

Figure 1. Internal structures and optical properties of core−shell and alloyed $CdSe_{1-x}Te_x$ quantum dots: (a) schematic drawings of four different types of quantum dots; (b) their corresponding fluorescence emission spectra. (1) Traditional core−shell CdTe−CdSe dots; (2) reversed core−shell dots; (3) homogeneous alloyed dots; and (4) gradient alloyed dots. All dots were synthesized to have a mean diameter of 5.9 nm (core plus shell) and an overall composition of $CdSe_{0.6}Te_{0.4}$, with relative standard deviations of ca. 10%. Within each batch of nanocrystal samples, the standard deviations for both size and composition were approximately 5%.

precise control of the Se:Te molar ratios. But the amount of injected cadmium is either in large excess or in short supply (by ca. 8-fold) relative to the total mole amounts of Se and Te. Under these conditions, the reagent in short supply would be completely consumed while the reagent in large excess would maintain a nearly constant concentration during the entire course of the reaction. From both kinetic analysis and experimental measurements, we show that alloyed quantum dots with a *homogeneous* internal structure can be prepared under *cadmium-limited* conditions and that alloyed dots with a *gradient* structure can be produced under *cadmium-rich* conditions (see schematics in Figure 1).

When a limited amount of cadmium is injected, the composition of the resulting nanocrystals is determined by the Se/Te molar ratio and by the different intrinsic Se and Te reactivities toward cadmium. The intrinsic reactivities are difficult to change without altering the experimental conditions, but the Se/Te ratio in the reaction mixture provides a convenient control parameter for preparing ternary quantum dots with a wide range of compositions. A key concept is that the quantum dot composition is determined only by the relative formation rates of CdSe and CdTe, not by the absolute cadmium concentration. The reason is that cadmium is a common species in both CdSe and CdTe, and its effect is dropped out in the kinetic equations describing the relative CdSe and CdTe reaction rates. Thus, the nanocrystal composition is expected to remain constant even when the cadmium concentration changes with reaction time, yielding a homogeneous alloy that is uniform from the particle core to the surface. Indeed, elemental analysis by inductively coupled plasma mass spectrometry (ICP-MS) at different growth intervals revealed an essentially constant composition as the particles grew from 2.0 to 8.0 nm (details below).

Under cadmium-rich conditions, on the other hand, the difference in the intrinsic Se and Te reactivity results in quantum dots with a gradient alloy structure. During rapid particle nucleation and growth in hot TOPO,[10,11] the initial core is rich in Te due to its faster reaction rate toward cadmium. As the free Te is being depleted from the reaction mixture, CdSe deposition becomes more important toward crystal growth. When all free Se and Te in the mixture are consumed particle growth will stop, yielding alloyed quantum dots with a gradient Te concentration from the core to the surface. Because the outer layer is largely made of CdSe, this layer acts as an encapsulating shell for the CdTe-rich core. But unlike the traditional core−shell nanocrystals synthesized in two sequential steps,[10,11] our gradient alloyed dots are prepared in a single step and do not have an abrupt boundary between the Te-rich core and the Se-rich shell. A potential problem not considered above is the so-called "Ostwald ripening" effect,[34,35] in which smaller particles or clusters are dissolved to feed the growth of larger ones. The net effect would be a composition averaging that renders the gradient dots more like the homogeneous dots. But this complication does not change the main conclusions of this work since growth is quenched before this mechanism becomes important.

Structure and Optical Properties. Figure 1 shows the schematic structures of four different types of semiconductor quantum dots and their fluorescence emission spectra. The traditional CdTe-core/CdSe-shell quantum dots (**1**) were synthesized by a two-step procedure, in which 4.5-nm CdTe cores were coated with a 0.7-nm CdSe shell. For the reverse core−shell structure (**2**), 4.9-nm CdSe quantum dots were coated with a 0.5-nm CdTe layer. At these core sizes and shell thicknesses, the core−shell dots of both types have the same overall diameter of 5.9 nm and the same elemental composition of 60% Se and 40% Te. Calculations based on either crystal lattice parameters or bulk CdSe and CdTe densities[33] yield composition results that are in excellent agreement (5%) with each other. Distinct from these core−shell structures, ternary alloyed quantum dots (**3**, homogeneous) were prepared by using cadmium oxide and an 8-fold excess of a 75:25 (molar ratio) Se:Te stock solution as discussed above. Under these reaction conditions, the resulting quantum dots were found to have an elemental composition of 60% Se and 40% Te, same as the core−shell structures. The size of the ternary quantum dots was controlled by the growth time, together with fine-tuning of the nucleation rate at slightly different temperatures. Using a new stock solution of 60% Se and 40% Te and an 8-fold excess of cadmium oxide, we prepared a second type of ternary alloyed quantum dots (**4**, gradient), for which the particle size was mainly controlled by the nucleation rate at different temperatures. The reaction was allowed to proceed to completion (all free Se and Te were consumed), but was stopped before significant Ostwald ripening took place, to prevent "defocusing" or broadening in the particle size distribution.[34] Thus, the gradient alloy dots have relatively narrow size distributions and the same Se:Te ratio as the stock solution.

With nearly identical sizes and compositions, we proceeded to examine how the internal structures (e.g., core−shell and

(34) Peng, X. G.; Wickham, J.; Alivisatos, A. P. *J. Am. Chem. Soc.* **1998**, *120*, 5343−5344.
(35) Desmet, Y.; Deriemaeker, L.; Parloo, E.; Finsy, R. *Langmuir* **1999**, *15*, 2327−2332.

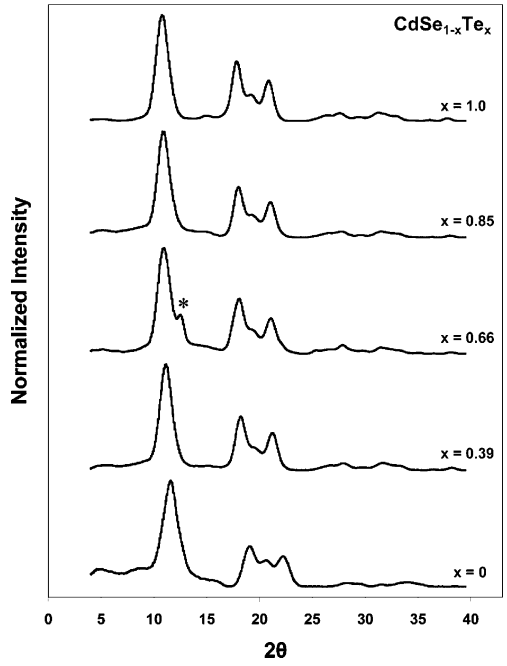

Figure 2. X-ray power diffraction data obtained from pure CdSe, pure CdTe, and alloyed $CdSe_{1-x}Te_x$ quantum dots. The size of all dots was approximately 5 nm in diameter, and the asterisk (*) indicates a spurious signal.

alloy) of quantum dots would influence their optical properties. As shown in Figure 1b, the core−shell CdTe−CdSe nanocrystals are intensely fluorescent (emission peak at 702 nm), but the reversed core−shell CdSe−CdTe quantum dots show little band-edge luminescence. This is not surprising because CdTe has a lower band gap than CdSe and does not provide an effective shell (leading to exciton recombination at surface trap sites). In comparison, both types of alloyed quantum dots are highly fluorescent, but their emission spectra are shifted to 741 nm for the gradient structure and to 757 nm for the homogeneous structure. Remarkably, the alloyed quantum dots exhibit similar fluorescence quantum yields (QE = 30−60%) and spectral widths (full width at half-maximum or fwhm = 35 nm) as the traditional core−shell dots (fwhm = 30−35 nm). The high quantum yields and narrow spectral widths indicate that the alloyed quantum dots do not contain a heterogeneous population of amorphous clusters but are highly crystalline in structure and monodisperse in size.

Powder X-ray diffraction data (Figure 2) confirm the crystalline wurtzite-type structure of the ternary particles. Broadened due to the finite nanocrystalline domain size, the wurtzite patterns of nanocrystals contain four peaks (a singlet peak at low angle and a triplet of peaks at high angle) whereas zinc blende patterns from nanocrystals only have two peaks (a singlet at low angle and a singlet at high angle).[36] The wurtzite structure is kinetically favored and is observed at all compositions of $CdSe_{1-x}Te_x$, ruling out the possibility of a phase change in the alloyed quantum dots.

Figure 3 shows results obtained from reaction kinetics, elemental composition, and transmission electron microscopy (TEM) studies. The kinetic data (a) indicate that the growth rate of CdTe is approximately double that of CdSe and that the

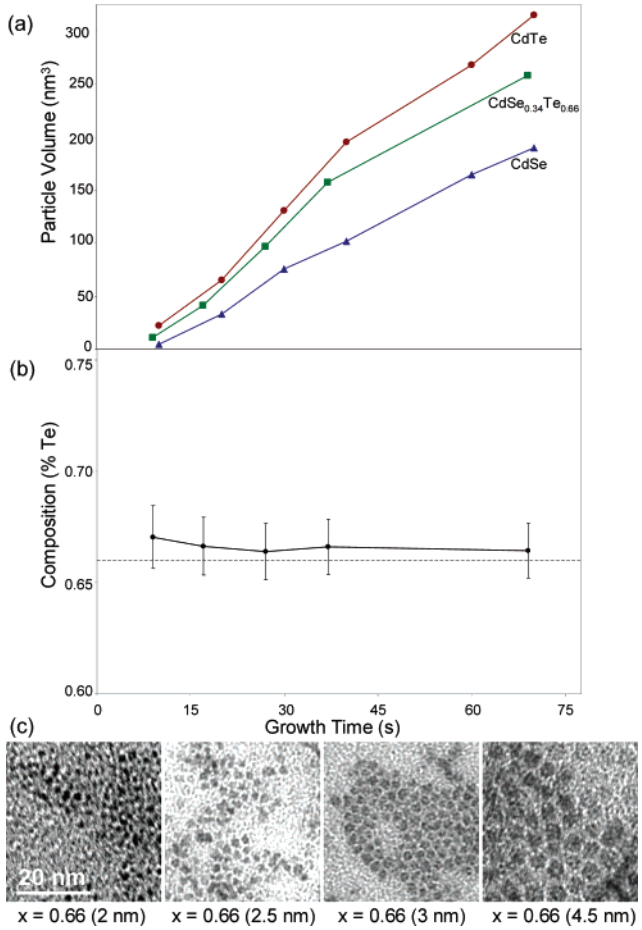

Figure 3. Growth kinetics, elemental composition, and TEM structural data obtained from homogeneous $CdSe_{0.34}Te_{0.66}$ quantum dots during nanocrystal growth: (a) plot of particle growth (volume) versus time; (b) plot of particle composition versus time; and (c) TEM images of alloyed quantum dots removed from the reaction mixture at different growth times. The symbol x is the mole fraction of tellurium in the alloy. See text for detailed discussion.

ternary dots grow at an intermediate rate depending on the exact composition and the reaction conditions. The elemental analysis data (b) reveal a nearly constant composition for the alloyed dots during the entire course of their growth. In fact, only a slight decrease of ca. 2% in Te composition was observed after extended periods of particle growth, during which the particle size increased from 2 to 8 nm. This decrease is reasonable because the total amount of Se and Te is only 8-fold in excess of cadmium (a finite number), so a small depletion will develop for Te with reaction time. This set of elemental data provides strong evidence that the ternary quantum dots have a homogeneous alloy structure that is nearly uniform from the start to the stop of particle growth. Furthermore, TEM data (c) demonstrate that at a constant composition of 66% Te excellent size controls and size monodispersity can be achieved for the ternary quantum dots. In fact, the elemental composition data are in excellent agreement with the theoretical values predicted from the stock Se/Te molar ratios and their kinetic rates. For example, we found that under cadmium-limited conditions injected Se/Te ratios of 75:25, 50:50, and 25:75 resulted in nanocrystal compositions of 61:39, 34:66, and 15:85, which are nearly identical to the predicted values of 60:40, 33:67, and 14:86.

(36) Tolbert, S. H.; Alivisatos, A. P. *Science* **1994**, *265*, 373−376. Tolbert, S. H.; Alivisatos, A. P. *Annu. Rev. Phys. Chem.* **1995**, *46*, 595−625.

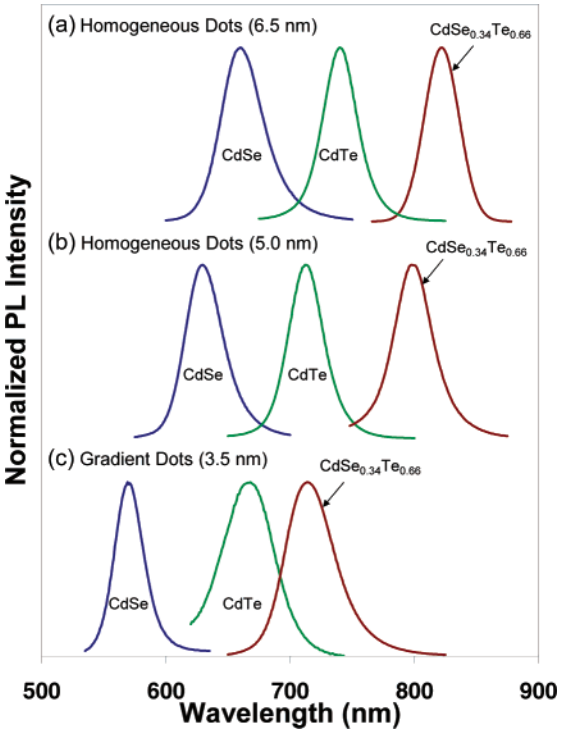

Figure 4. Comparison of the emission spectra among CdSe, CdTe, and $CdSe_{0.34}Te_{0.66}$ quantum dots at three particle sizes. For each size series (a)−(c), the binary dots and the alloyed dots (either homogeneous or gradient) were synthesized to have the same overall diameter (accurate to within 5−10%).

Evidence for the alloyed internal structures also comes from the finding that the quantum dots can be tuned to emit light outside of the wavelength range defined by the binary CdSe and CdTe nanocrystals. Figure 4 shows the fluorescence spectra obtained from three size series of CdSe, CdTe, and $CdSe_{1-x}Te_x$ quantum dots. In the 3.5-nm size series, the gradient alloyed dots emit fluorescent light that is 145 nm longer than the binary CdSe dots and 50 nm longer than the binary CdTe dots. In the 5.0-nm and 6.5-nm size series, the emission spectra of the homogeneous alloyed dots are red-shifted to ca. 800 and 825 nm, respectively. In each of these size series, the particle sizes are constant within 5−10%, as judged by the TEM data (Figure 5). In the worst case scenario, the size of the CdTe dots would be 10% larger than the mean (5.0 nm) and the size of the CdSeTe dots would be 10% smaller than the mean. The emission wavelength of the largest CdTe dots (5.5 nm) is expected to be 730 nm, which is still shorter than the emission peak (780 nm) of the smallest $CdSe_{0.34}Te_{0.66}$ dots (4.5 nm). This simple statistical analysis rules out particle size variations as the cause of the large spectral shifts observed in Figure 4.

Further studies of the core−shell and alloyed structures might be carried out by using high-resolution quantitative X-ray photoelectron spectroscopy (XPS), because the escape depth of photoelectrons is dependent on both the emission energy and the shell thickness. Previous research by Cao and Banin[12] has shown that the XPS ratio data are distinctly different for core−shell and alloyed InAs−ZnS nanocrystals. But for the core−shell and alloyed InAs−InP quantum dots (which are similar to the CdSe−CdTe structures studied in this work), the escape depth data are much less convincing. We believe that our elemental analysis results and the observed novel optical properties, together with the fact that CdSe and CdTe form alloys at all proporations, have provided compelling evidence for the proposed alloy structures of the ternary CdSeTe quantum dots.

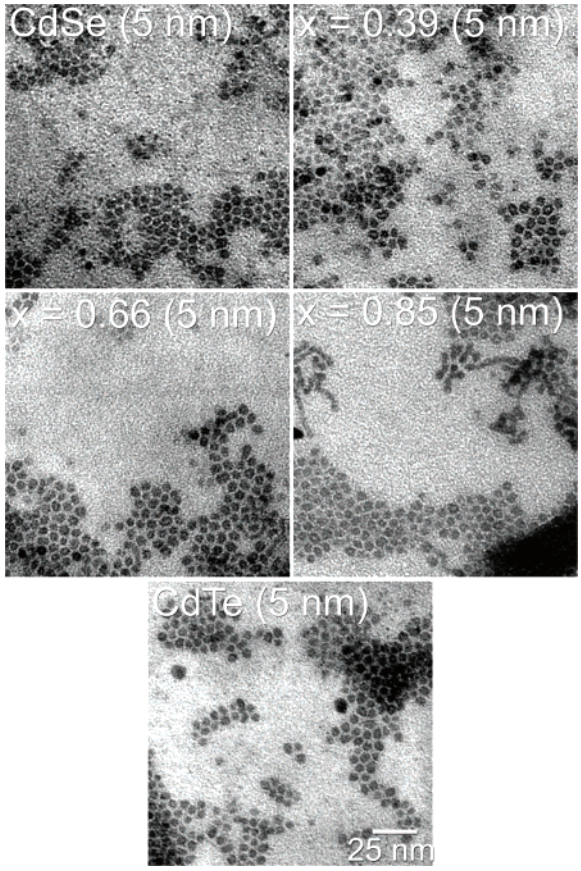

Figure 5. Transmission electron microscopy (TEM) images of a series of $CdSe_{1-x}Te_x$ quantum dots (x = 0, 0.39, 0.66, 0.85, 1.0) showing their approximately constant size (5 nm).

Nonlinear Composition Effect. To investigate the composition effect in a more quantitative manner, we have prepared and characterized alloyed quantum dots in a broad range of sizes and compositions. Figure 6 compares the absorption and fluorescence spectra for these dots and further shows the relationships between the composition and the absorption/emission energies. The bulk data are also included for comparison.[33] The absorption and emission data show several resolved electronic transitions and clear band-edge fluorescence emission, similar to those reported for high-quality binary quantum dots,[29,32] The plots, however, reveal a striking nonlinear relationship between the composition and the excitonic absorption and band-edge emission. There is no doubt that this nonlinear relationship clauses the unusually large spectral shifts reported in Figure 4. In fact, alloyed quantum dots with a tellurium composition between 30% and 100% should emit light at longer wavelengths than the parent CdSe and CdTe dots. Also, it is clear that the homogeneous alloyed dots of all sizes follow a similar nonlinear curve, reaching the lowest energy or the "depression" point at ∼60% tellurium content.

It is worth noting that the Vegard's Law for bulk and thin film alloy materials is a linear function: $E_{alloy} = xE_A + (1 - x)E_B$, where x is the mole fraction, E_A, E_B, and E_{alloy} are the band gap energy (or other properties) of pure A, pure B, and the alloy A_xB_{1-x}, respectively.[37] This law has been

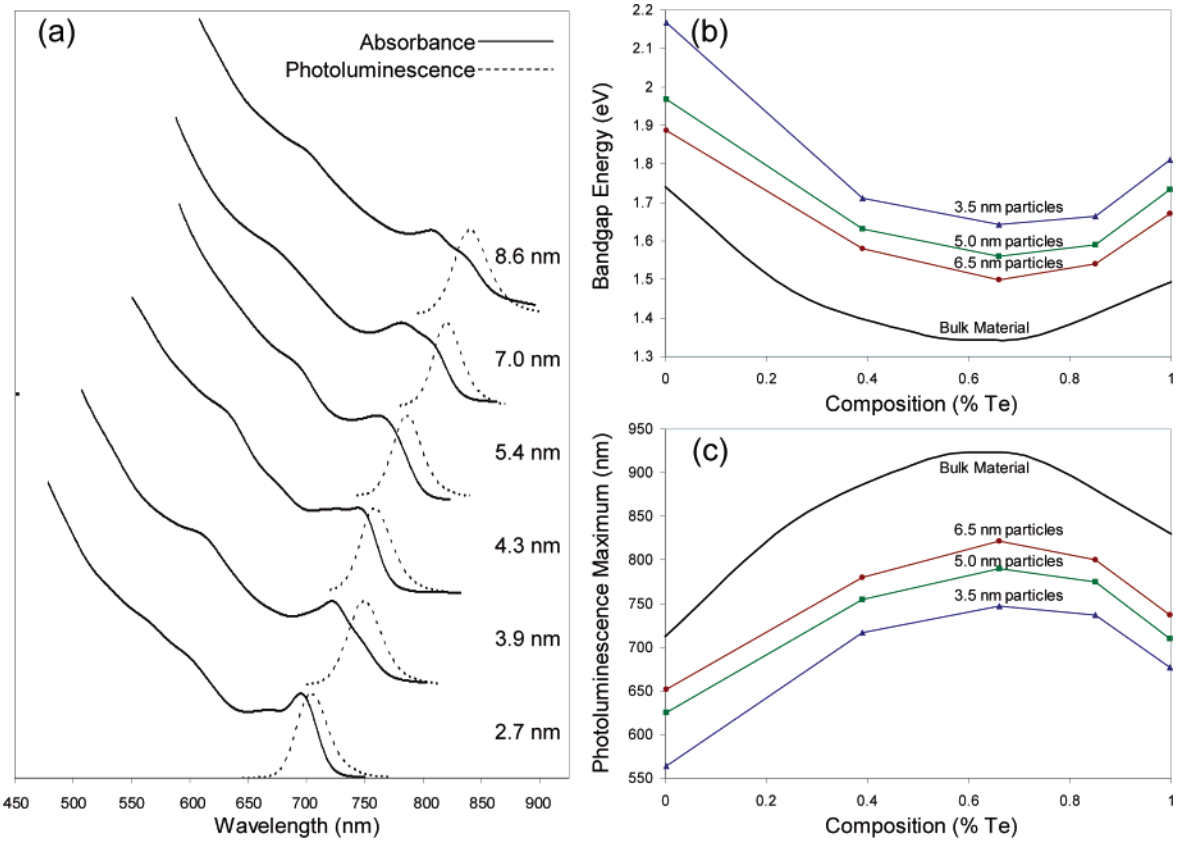

Figure 6. Relationship between the composition and the absorption/emission energies for homogeneous $CdSe_{1-x}Te_x$ quantum dots at different sizes: (a) UV−vis absorption and photoluminescence spectra of $CdSe_{0.34}Te_{0.66}$ quantum dots in the size range of 2.7−8.6 nm; (b) plots of the absorption onset energy (in eV) as a function of tellurium content; and (c) plots of the emission peak wavelength (nm) as a function of tellurium content. Note that the absorption onsets are slightly lower in energy than the emission maxima.

successful in predicting the structure and function of many alloyed materials. For example, the optical absorption spectra of bimetallic Ag_xAu_{1-x} nanoparticles follow a strictly linear relationship with alloy composition.[38−40] However, this linear relationship is only a first approximation and is not strictly obeyed in several classes of semiconductor alloys. In particular, previous studies of bulk CdSeTe alloys have found a very strong nonlinear effect, called "optical bowing".[33,41] Thus, the nonlinear effect observed in alloyed semiconductor nanocrystals is not caused by quantum confinement per se, although size confinement could be a contributing factor.

We believe that similar mechanisms are operative in both the macroscopic and nanoscopic alloys. According to a theoretical model developed by Zunger and co-workers,[42,43] the observed nonlinear effect arises from three structural and electronic factors: (i) different ions in the alloy have different atomic sizes, (ii) these ions have different electronegativity values, and (iii) the binary structures have different lattice constants. It is believed that relaxation of the anion−cation bonds to their equilibrium positions leads to local structural ordering and a particularly large band gap reduction in CdSeTe-type semiconductor alloys. This theory has been remarkably successful in explaining and predicting the nonlinear compositional effect for bulk materials.

Band Gap Engineering and Bioimaging. Bulk alloying has been used to developed high-strength materials for mechanical applications (e.g., aircrafts), biocompatible materials for medical implants, and a broad range of semiconductor materials for optoelectronic applications (e.g., diode lasers and detectors). For alloyed nanostructures, our results demonstrate that three factors (particle size, composition, and internal structure) can be used to control the quantum confinement effect, providing new or novel properties not available from individual components. This insight opens the possibility of developing a variety of ternary and quaternary semiconductor quantum dots based on both II−VI and III−VI materials.[33]

Due to their far-red and near-infrared fluorescence properties, the alloyed quantum dots are well suited for applications in in vivo molecular imaging[44−48] and ultrasensitive biomarker detection.[49,50] Visible light has been used for cellular imaging and tissue diagnosis,[51,52] but optical imaging of deeper tissues

(37) Vegard, L. *Z. Physik* **1921**, *5*, 17−26.
(38) Mulvany, P. *Langmuir* **1996**, *12*, 788−800.
(39) Link, S.; Wang, Z. L.; El-Sayed, M. A. *J. Phys. Chem. B* **1999**, *103*, 3529−3533.
(40) Mallin, M. P.; Murphy, C. J. *Nano Lett.* **2002**, *2*, 1235−1237.
(41) Poon, H. C.; Feng, Z. C.; Feng, Y. P.; Li, M. F. *J. Phys.: Condens. Matter* **1995**, *7*, 2783−2799.
(42) Bernard, J. E.; Zunger, A. *Phys. Rev. B* **1987**, *36*, 3199−3226.
(43) Wei, S. H.; Zhang, S. B.; Zunger, A. *J. Appl. Phys.* **2000**, *87*, 1304−1311.
(44) Weissleder, R.; Tung, C. H.; Mahmood, U.; Bogdanov, Jr. *Nature Biotechnol.* **1999**, *17*, 375−378.
(45) Bremer, C.; Tung, C. H.; Weissleder, R. *Nat. Med.* **2001**, *7*, 743−748.
(46) Becker, A.; Hessenius, C.; Licha, K.; Ebert, B.; Sukowski, U.; Semmler, W.; Wiedenmann, B.; Grotzinger, C. *Nat. Biotechnol.* **2001**, *19*, 327−331.
(47) Zaheer, A.; Lenkinski, R. E.; Mahmood, A.; Jones, A. G.; Cantley, L. C.; Frangioni, J. V. *Nat. Biotechnol.* **2001**, *19*, 1148−1154.
(48) Sevick-Muraca, E. M.; Houston, J. P.; Gurfinkel, M. *Curr. Opin. Chem. Biol.* **2002**, *6*, 642−650.
(49) McWhorter, S.; Soper, S. A. *Electrophoresis* **2000**, *21*, 1267−1280.
(50) Patonay, G.; Antoine, M. D. *Anal. Chem.* **1991**, *63*, A321−A326.
(51) Sokolov, K.; Follen. M.; Richards-Kortum, R. *Curr. Opin. Chem. Biol.* **2002**, *6*, 651−658.

(millimeters) requires the use of far-red and near-infrared light in the spectral range of 650−900 nm. This wavelength range provides a "clear" window for in vivo optical imaging because it is separated from the major absorption peaks of blood and water. In comparison with traditional organic fluorophores,[44−52] near-infrared-emitting quantum dots should allow more sensitive biomolecular detection and multicolor optical imaging. Under photon-limited in vivo conditions (where light intensities are severely attenuated by scattering and absorption), the large absorption coefficients of quantum dots (on the order of 10^6 cm^{-1} M^{-1}, ca. 10−20 times larger than those of common organic dyes) will be essential for efficient probe excitation. Unlike current single-color molecular imaging, multiwavelength optical imaging with quantum dots will allow intensity ratioing, spatial colocalization, and quantitative target measurements at single anatomical structures such as single metastasized tumor sites.

For these biological applications, we note that the alloyed quantum dots can be made water-soluble and biocompatible by using the surface-modification and cross-linking procedures reported for CdSe and CdTe binary quantum dots.[3−8] When solubilized with mercaptoacetic acid and coated with a biopolymer or a synthetic polymer,[53] the ternary dots are found to exhibit excellent optical properties such as narrow spectral width, high quantum yields, and excellent photostability, similar to those of high-quality binary nanocrystals.

In conclusion, we have reported a novel procedure for preparing large quantities of alloyed semiconductor quantum dots (CdSeTe) for continuous tuning of quantum confinement without changing the particle size. In addition to particle size, our results demonstrate that two new parameters, composition and internal structure, are available for tuning the optical and electronic properties of alloyed semiconductor quantum dots. The concept of composition tuning is of course not new, but we have achieved perhaps the first demonstration of how this concept works in a colloidal semiconductor system. With broadly tunable optical and electronic properties, this new class of alloyed quantum dots should open exciting possibilities in designing novel nanostructures and in developing near-infrared-emitting probes for multiplexed optical encoding and in vivo molecular imaging.[54,55]

Acknowledgment. We acknowledge Joseph B. Strausburg, Scott Robinson, John C. Bollinger, and Denise McClenathan of Professor Gary M. Hieftje's group (Indiana University—Bloomington) for technical help in sample synthesis and characterization. We are also grateful to Dr. Robert P. Apkarian and the Integrated Microscopy and Microanalytical Facility (IMMF) for TEM studies. This work was supported by grants from the National Institutes of Health (R01 GM60562) and the Coulter Translational Research Program at Georgia Tech and Emory University.

JA035000O

(52) Brown, E. B.; Campbell, R. B.; Tsuzuki, Y.; Xu, L.; Carmeliet, P.; Fukumura, D.; Jain, R. K. *Nat. Med.* **2001**, *7*, 866−870.
(53) Gao, X.; Chan, W. C. W.; Nie, S. M. *J. Biomed. Opt.* **2002**, *7*, 532−537.
(54) Han, M. Y.; Gao, X. H.; Su, J. Z.; Nie, S. *Nat. Biotechnol.* **2001**, *19*, 631−635.
(55) Chan, W. C. W.; Maxwell, D. J.; Gao, X.; Bailey, R. E.; Han, M.-Y.; Nie, S. *Curr. Opin. Biotechnol.* **2002**, *13*, 40−46.